Sol-gel Approach in Molecular Imprinting for Crystal Violet Selective Recognition
(Pendekatan Sol-gel dalam Peneraan Molekul untuk Pengecaman Memilih Kristal Ungu)

SALIZA ASMAN*, SHARIFAH MOHAMAD & MOHD KAMARULZAKI MUSTAFA

ABSTRACT

A limitation of conventional MIP in thermal and mechanical stabilities condition, improper porosity and low adsorption capacity, give a reason to introduce a sol-gel method in molecular imprinting process recently. In this study, a synthesis of new sol-gel molecularly imprinted polymer (SG-MIP) was studied for crystal violet (CV) selective recognition. The control non-molecularly imprinted polymer (SG-NIP) was also synthesized as reference. The preparation of SG-MIP was introduced by a combination of the organic and inorganic mixture. The organic solution included the methacrylic acid, trimethylolpropane trimethacrylate, and benzoyl peroxide which are monomer, crosslinker, and initiator, respectively. The inorganic solution involved the ratio of tetraethyl orthosilicate: ethanol (1:1 v/v). The functional group analysis proved the successful synthesized SG-MIP and SG-NIP. The thermal analysis indicated high thermal stability for SG-MIP and SG-NIP, respectively. The morphology and surface analyses showed the respective different structures, surface, and porosity values between SG-MIP and SG-NIP, which influence the selectivity study and adsorption behaviour of SG-MIP toward CV adsorption. The result verified that the SG-MIP (4.900 mgg^{-1}) has higher adsorption and higher selectivity characteristics compared to SG-NIP (4.432 mgg^{-1}). The equilibrium data of kinetic and isotherm studies for SG-MIP and SG-NIP were well-fitted to the pseudo-second order model ($R^2 = 0.9997$ and $R^2 = 0.9996$) and Freundlich isotherm model ($R^2 = 0.9500$ and $R^2 = 0.9764$), respectively. The Freundlich isotherm was supported by the Scatchard plot instead of the Langmuir isotherm model.

Keywords: Crystal violet; Freundlich isotherm; Langmuir isotherm; sol-gel method

ABSTRAK

Batasan MIP konvensional dalam keadaan kestabilan terma dan mekanikal, keliangan yang tidak sesuai dan kapasiti penjerapan yang rendah, memberi alasan untuk memperkenalkan kaedah sol-gel dalam proses pencetakan molekul baru-baru ini. Dalam kajian ini, satu sintesis polimer bercirikan molekul sol-gel baru (SG-MIP) dikaji untuk pengecaman memilih kristal ungu (CV). Polimer cetakan bukan molekul kawalan (SG-NIP) juga disintesis sebagai rujukan. Penyediaan SG-MIP diperkenalkan dengan gabungan campuran organik dan bukan organik. Penyelesaian organik tersebut merangkumi asid metakrilik, trimetilolpropana trimetakrilat dan benzoil peroksida yang masing-masing adalah monomer, penghubung silang, dan pemula. Larutan bukan organik melibatkan nisbah tetraetil ortosilika: etanol (1: 1 v/v). Analisis kumpulan berfungsi membuktikan SG-MIP dan SG-NIP yang berjaya disintesis. Analisis terma menunjukkan kestabilan terma yang tinggi masing-masing untuk SG-MIP dan SG-NIP. Analisis morfologi dan permukaan menunjukkan struktur, permukaan, dan nilai keliangan yang berbeza antara SG-MIP dan SG-NIP, yang mempengaruhi kajian memilih dan tingkah laku penjerapan SG-MIP terhadap penjerapan CV. Hasilnya mengesahkan bahawa SG-MIP (4.900 mgg^{-1}) mempunyai penjerapan yang lebih tinggi dan ciri pemilihan yang lebih tinggi berbanding dengan SG-NIP (4.432 mgg^{-1}). Data keseimbangan kajian kinetik dan isoterma untuk SG-MIP dan SG-NIP sesuai dengan model pesanan pseudo-kedua ($R^2 = 0.9997$ dan $R^2 = 0.9996$) dan model isoterma Freundlich ($R^2 = 0.9500$ dan $R^2 = 0.9764$. Isoterma Freundlich disokong oleh plot Scatchard dan bukannya model isoterma Langmuir.

Kata kunci: Isoterma Freundlich; isoterma Langmuir; kaedah sol-gel; kristal ungu

INTRODUCTION

Molecularly imprinted polymer (MIP) is a well-known polymeric network designed from the molecular imprinting technology (MIT). The MIP material is structured by copolymerizing the functional monomers and crosslinker monomers in the existence of the template analyte. The functional monomer molecules form a complex with template molecules when the active functional groups are adjoined together and assembled with the strongly cross-linked polymeric structure. Later the imprint template molecule was removed from the MIP network matrix, leaving the MIP with good formation of complementary binding sites in shape and size to the imprint molecule (Ertürk & Mattiasson 2017).

However, general MIP deteriorates from thermal stability and mechanical stability conditions, thus provides the improper porosity and poor adsorption capacity. For this reason, the combination of MIT and sol-gel method technology is tremendously interesting and have significant attention, thus becoming a growing area of research, recently. The sol-gel method is a versatile method that can prepare a gel form from liquid solution at ambient processing conditions. Besides, it involves the mixing of inorganic precursors of metal alkoxide with water and solvent in the existence of an acid/base catalyst (Kessler 2018).

Many advantages are boosted on MIP prepared by sol-gel method than general MIP methods. The SG-MIP is synthesized under mild conditions without required heat or radiation to polymerize, especially dealing with thermal and photosensitive template molecules. Besides, the utmost of imprinting polymer synthesis participates in the media of organic monomer-solvent system, but it is lack with water compatibility. Hence, the synthesis of MIP *via* the sol-gel method in aqueous/alcoholic mixtures media is possible. Thus, the sol-gel method is a proposing alternative MIP polymerization process not only simple, manageable, and low-cost method but capable to serve the MIP fabrication with excellent well-ordered porosity and high surface area, selectivity, capacity, and thermal stability.

A crystal violet (CV) molecule was chosen in this study as a template for sol-gel molecularly imprinted polymeric matrix. CV is belonging to the cationic triphenylmethane group dyes. It is major used in the textile industry and widely used for several purposes for instance as a dermatological agent, medicine for the veterinary field, and biological stain (Kulkarni et al. 2017; Kumar & Ahmad 2011). However, it is well-known a mutagenic and carcinogenic which can give harmful effects through ingestion, skin contact, and inhalation, thus, causing several diseases such as severe eye irritation and serious cancer to human beings (Lellis et al. 2019).

In the molecular imprinting research, few approaches to imprint CV have been described in an organic polymer. Also, several reports are available in the literature for the imprinting by a sol-gel method with various compounds. However, to the best of our knowledge, the study on sorption of CV by SG-MIP has yet been reported. The goal of this work is to synthesize and characterize a new sol-gel molecularly imprinted polymer (SG-MIP) for selective recognition of CV as a template by applying a sol-gel method technology to the molecular imprinting technology. A similar non-sol-gel molecularly imprinted polymer (SG-NIP) was prepared by omitting the additional template molecule. The adsorption behaviour of CV by SG-MIP in kinetic and isotherm parameters was explored.

MATERIALS AND METHODS

Methacrylic acid (MAA) 99.0%, benzoyl peroxide (BPO) 98.0%, trimethylolpropane trimethacrylate (TRIM; contains 250 ppm monomethyl ether hydroquinone as inhibitor, technical grade), tetraethyl orthosilicate (TEOS) 99.9%, ethanol (EtOH), methanol (MeOH), hydrochloric acid (HCl), acetic acid (CH_3COOH), crystal violet (CV; molecular weight: 407.99 g/mol) 90.0%, methylene blue (MB; molecular weight: 319.86 $gmol^{-1}$) 97.0%, and methylene orange (MO; molecular weight: 327.33 $gmol^{-1}$) 85.0% were supplied by Sigma-Aldrich (Switzerland).

SYNTHESIS OF SOL-GEL MOLECULARLY IMPRINTED POLYMER (SG-MIP)

A procedure was adopted by Kia et al. (2016) with a small alteration, two different solutions were prepared which are inorganic solution and organic solution. The inorganic solution was prepared with the hybridization process whereas TEOS/EtOH (1:1 v/v; 1.35:1.35 mL) were mixed and stirred for 10 min. Then, 50 mg of CV as a template and diluted HCl (12.5% (v/v), 0.8 mL) was added into the mixture and stirred at 50 °C, thus obtaining the sol. The organic solution was prepared by mixing 10 mmol of MAA as a monomer, 9.61 mmol of TRIM as a crosslinker, and 0.25 mmol of BPO as initiator. The mixture was stirred at 50 °C for 20 min. The organic solution was added dropwise into the inorganic solution and stirred at 50 °C for an hour. Lastly, the mixture was kept for 48 h to form an *in-situ* gel network.

The SG-MIP product was then crushed, ground, and sieved thus, obtaining a tiny and irregular size particle. Then, the extraction process was applied to remove the template molecule from the SG-MIP particles network was carried out for the resulting SG-MIP particles. The unreacted monomers and impurities compounds were also spontaneously. The extraction process was prepared with the methanol/acetic acid mixture (9:1 v/v) by using a Soxhlet extraction system. The template removal was ensured by evaluating the absorbance of the template repetitively until the negligible CV concentration could not be detected in the elution at 582 nm by the UV-Vis Spectrophotometer. The rancid smell of acetic acid through SG-MIP particles was eliminated with distilled water by a repetitively washing process. Finally, the SG-MIP particles were dried at 80 °C under vacuum and kept in a desiccator. A similar procedure was conducted for synthesizing sol-gel non-imprinted polymer (SG-NIP) by omitting the template involved.

This procedure shows the matrix of SiO_2 encapsulates the CV molecule under acid-catalyzed mediums. Then, it was polymerized around with the organic polymer which contains monomer, crosslinker, and initiator. The template binding sites were formed after the template was removed from SG-MIP. Thus, the resultant polymeric SG-MIP has potential recognition cavities that are matching to the shape, size, and chemical functionality of the CV molecule.

CHARACTERIZATION

The SG-MIP and SG-NIP were characterized by using Perkin Elmer spectrum 100 Fourier transform infrared (FTIR) spectroscopy (USA) and JOEL, JSM 7600F field emission scanning electron microscope (FESEM) (Japan) for analyzing the functional group and the morphology structures, respectively. The thermal gravimetric analysis curves were inspected by using TA Instruments Q500, Perkin Elmer thermal gravimetric analyzer (TGA) (USA). The constant heating rate was fixed at 20 °C per min in the range of 50-900 °C in a flow of nitrogen gas. The XRD characterization was conducted by using X-ray powder diffraction (XRD) (Model Bruker D8 Advance, USA). The measurement of polymers surface and porosity were determined by using Quantachrome surface area analyser (USA). The rebinding study based on adsorption and selectivity experiments were determined by using Perkin Elmer Lambda 900 UV-vis/NIR ultraviolet-visible spectroscopy (UV-Vis) spectrophotometer (USA).

SELECTIVITY ANALYSIS

A 0.05 g of SG-MIP and SG-NIP were mixed separately with 20 mL of CV solution (10 mgL^{-1} concentration). The mixture was incubated at ambient temperature for an hour. After the period, the final concentration of the elution was detected using the UV-Vis spectrophotometer. The quantity of substrate-bound (Q) to SG-MIP or SG-NIP was computed following (1):

$$Q \ (mgg^{-1}) = V \ (C_i - C_f) \qquad (1)$$

with represents, C_i and C_f (mgL^{-1}) is the initial and final concentrations of the substrate solution. The V (L) is the volume of the solution (Esfandian et al. 2012).

KINETIC STUDY

The kinetic adsorption study of SG-MIP and SG-NIP were evaluated with the time interval (5, 10, 15, 30, 60, 90, 120, 150, and 180 min) at ambient temperature. 0.05 g of SG-MIP or SG-NIP were mixed with 20 mL of CV solution (10 mgL^{-1} of CV concentration) and incubated for each time interval stated. Each test was carried out triplicate as parallel experiments. The CV absorption at a time (t) is the binding capacity, and q_t (mgg^{-1}) was computed by (2):

$$q_t = [(C_o - C_t) \times v]/w \qquad (2)$$

with q_t (mgg^{-1}) is the binding capacity of SG-MIP or SG-NIP; C_o (mgL^{-1}) is the initial solutions and C_t (mgL^{-1}) is any time of CV solutions (mgL^{-1}). While, v (L) is the volume of CV solution; and w (g) is the mass of polymers.

ADSORPTION KINETICS

The sorption kinetics parameter of SG-MIP and SG-NIP was studied by pseudo-first order and pseudo-second order. The equation of pseudo-first order hypothesizes the change rate of solute adsorbed with time, is directly proportional to the variance of saturated concentration and the amount of solid adsorbed with time, as expressed by (3) as follow (Binupriya et al. 2010):

$$\log (q_e - q_t) = \log \ q_e - \frac{k_1 t}{2.303} \qquad (3)$$

with q_e (mgL^{-1}) and q_t (mgL^{-1}) is the amount of adsorbate adsorbed at equilibrium and at a time (t), respectively. k_1 (min^{-1}) is the pseudo-first order rate constant determines from the slope. The value of log ($q_e - q_t$) is graphed against t. While q_e value is identified from the plot's intercept.

This model is applicable when the calculated q_e value is comparable with the experimental value data.

Pseudo-second order visualizes the adsorption behaviour, which is promising with an adsorption mechanism presence the rate-controlling steps. The pseudo-second order model is denoted as (4):

$$\frac{t}{q_t} = \frac{1}{h} - \frac{t}{q_e} \tag{4}$$

with h = k_2 q_e^2 (mgg^{-1} min^{-1}) and k_2 (gmg^{-1} min^{-1}) are the sorption rate at initial and rate constant of pseudo-second order kinetic, respectively. The k_2 values are calculated from the slope. While the q_e values are identified from the intercept of the graph t/q_t versus t. The $t_{1/2}$ (min) values are the half-time necessary for the adsorption to take as considerably compound as at equilibrium values. The equation (5) is as follows:

$$t_{1/2} = \frac{1}{k_2 q_e} \tag{5}$$

ISOTHERM STUDY

The adsorption isotherm was studied with several concentrations of CV (10, 50, 100, 150, 200, and 250 mgL^{-1}) at ambient temperature using the optimized time. The mixture of 20 mL of CV solution with 0.05 g of SG-MIP or SG-NIP was incubated and shaken by using a mechanical shaker. Each test was carried out triplicate. The binding capacity, q_e (mgg^{-1}) of CV uptake at equilibrium was computed using (6):

$$q_e = [(C_o - C_e) \times v]/w \tag{6}$$

with q_e (mgg^{-1}) is the binding capacity of SG-MIP or SG-NIP. C_o is the initial and C_e is the equilibrium concentration of CV solutions (mgL^{-1}), respectively. The CV solution volume is symbolized as v (L). The mass of SG-MIP particle dosage is symbolized as w (g). The sorption isotherms parameter of SG-MIP and SG-NIP was studied by Langmuir and Freundlich isotherms models.

Langmuir isotherm model is demonstrative of monolayer adsorption arising with a dynamically uniform surface and the adsorbed molecules are not interactive. When the monolayer is entirely saturated, the equilibrium is successfully achieved. It is definite by (7):

$$\frac{C_e}{q_e} = \frac{C_e}{q_m} + \frac{1}{b q_m} \tag{7}$$

with C_e (mgL^{-1}) is the concentration of adsorbate in equilibrium. q_m (mgL^{-1}) is the maximum sorption capacity. (mgL^{-1}) is the Langmuir constant. The Langmuir constant (q_m) is correlated to the monolayer adsorption capacity. The values of b are the adsorbent affinity towards adsorbate. The prediction of adsorption efficiency can evaluate with the dimensionless equilibrium parameter as (8) (Asman et al. 2015b):

$$R_L = \frac{1}{1 + b C_0} \tag{8}$$

with C_0 (mgL^{-1}) is the adsorbate concentration at initial. The separation factor, R_L value specifies the adsorption of the isotherm: $R_L > 1$ (unfavourable), $R_L = 1$ (linear), 0 $< R_L < 1$ (favourable), $R_L = 0$ (irreversible).

Freundlich isotherm model defines the multilayer adsorption on a dynamically heterogeneous surface and adsorbed molecules are interactive (Torres-Caban et al. 2019). The model is linearized to give (9):

$$\log q_e = \log C_e \left(\frac{1}{n}\right) + \log K_f \tag{9}$$

with n is the Freundlich constant for intensity and K_f (mgL^{-1}) is sorption capacity. The values of K_f is determined from the slope, and the values of n are determined from the plot's intercept of $\log q_e$ versus $\log C_e$.

SCATCHARD PLOT

Scatchard equation is known to be sensitive to heterogeneous and cooperative binding effects. The equation 10 is:

$$\frac{Q_e}{C_e} = \frac{Q_m - Q_e}{K_d} \tag{10}$$

with Q_e (mgg^{-1}) is the capacity of equilibrium adsorption; C_e (mgL^{-1}) is the equilibrium concentration of CV; (mgg^{-1}) is the maximum capacity of adsorption the SG-MIP and SG-NIP; and K_d (mgL^{-1}) is the equilibrium dissociation constant.

RESULTS AND DISCUSSION

FUNCTIONAL GROUP ANALYSIS

The FTIR spectra (Figure 1) of SG-MIP, SG-NIP, TEOS, and MAA. The spectrum of MAA recorded a band at 2963.42 and 2930.76 cm^{-1} indicated O-H stretching, and a band at 1454.95, 1428.28, and 1375.92 cm^{-1} presented for

O-H bending which confirming the presence of carboxylic acid groups. The hydrogen bonding of carboxylic acid caused a broad and sharp peak. The band at 1689.92 and 1633.48 cm⁻¹ are assigned for stretching vibration of the carbonyl groups, C=O. The other bands are observed for C-O stretching at 1297.06 and 1202.15 cm⁻¹. Around 1008.15, 809.48, 651.79 and 553.73 cm⁻¹ indicate C-H bending vibrations.

TEOS spectrum presents a band at 2975.84, 2929.69 and 2890.20 cm⁻¹ indicated the existence of unreacted TEOS in the silica particles. A band at around 1442.82, 1366.26, and 1391.24 cm⁻¹ presented for the Si-O-C bond. While around 1100.06, 1073.95, and 784.37 cm⁻¹ to 959.00 cm⁻¹ considered the main characteristic peaks of Si-O-C and C-O-C and Si-O-H bonds bending vibrations. It can be presented to the stretching modes of the siloxane framework, Si-O-Si. The spectra of SG-MIP and SG-NIP have different characteristics. The SG-MIP shows rough

bands at 3847.52 and 3741.85 cm⁻¹ which can be showed to the intermolecular bond that occurs between the amine groups of CV with a carboxylic acid group of MAA. The bands at 3445.61 cm⁻¹ (SG-MIP) and 3445.14 cm⁻¹ (SG-NIP) were recorded to the existence of alcohol O-H stretching. The wide band at wavenumbers of 2919.98 cm⁻¹ (SG-MIP) and 2919.85 cm⁻¹ (SG-NIP) assigned to C-H stretching confirming the O=C-H groups.

Additionally, two significant bands at 1727.10 cm⁻¹ (SG-MIP) and 1730.15 cm⁻¹ (SG-NIP) assigned to C=O stretching showed the existence of TRIM crosslinker. The other bands are also observed such as C-H bending at 1384.70 cm⁻¹ (SG-MIP) and 1384.63 cm⁻¹ (SG-NIP). The band around 1151 cm⁻¹ in SG-MIP contributed from C-O-C saturated ester stretching vibration suggested the copolymerization of TRIM and MAA in the polymerization process is successful.
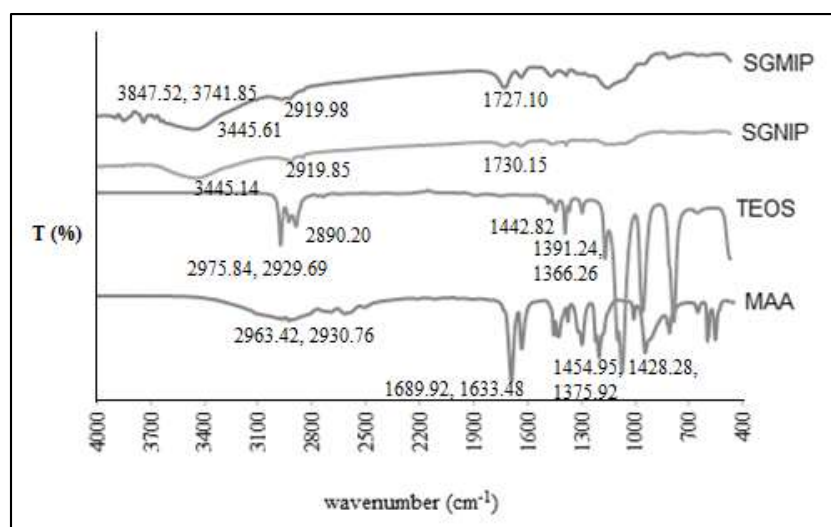
FIGURE 1. FTIR spectra of (a) SG-MIP (b) SG-NIP (c) TEOS and (d) MAA

MORPHOLOGY ANALYSIS

The morphologies of SG-MIP and SG-NIP particles (Figure 2) were analyzed by using FESEM with 50,000x magnifications. The morphology of polymers shows substantial different morphologies. SG-MIP has rough with a densely packed, loose, smooth and a bit porous surface. This morphology could expect having minute interstices through which liquid may pass. This existence was caused by the dissolution and extraction of the CV molecules from the SG-MIP matrix. This morphological structure is found

nearly similar with the synthesis of MIP by Asman et al. (2015a) and Wang et al. (2019). SG-NIP surface contains a rougher configuration, pores, and less dense than SG-MIP. This observation is most likely due to the repetitive extraction and washing steps for removing impurities instead of no specific binding site that was created inside the SG-NIP matrix. The difference in polymers morphology may account for the greater efficiency found for the SG-MIP polymer.
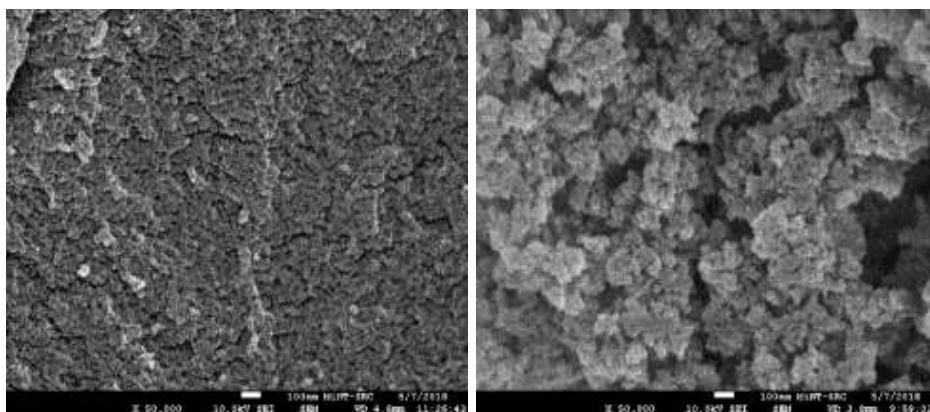
FIGURE 2. Morphological images of (a) SG-MIP and (b) SG-NIP

THERMAL ANALYSIS

A Thermogravimetric (TG) curves are recorded for SG-MIP and SG-NIP in Figure 3 with a similar trend. The TG curves of both polymers show a small weight loss within 100 °C, possibly to the loss of free water from the polymers content. The mass proportion of free water is approximately 3%. The higher mass loss for SG-MIP and SG-NIP is observed in the range of 150 to 450 °C. This temperature range can be considered the stage of mass loss of imprinted polymer layers. No loss of mass was observed after 500 °C. Furthermore, the TGA result indicates that the polymers have the highest thermal decomposition value of 550 °C which remained virtually the same.
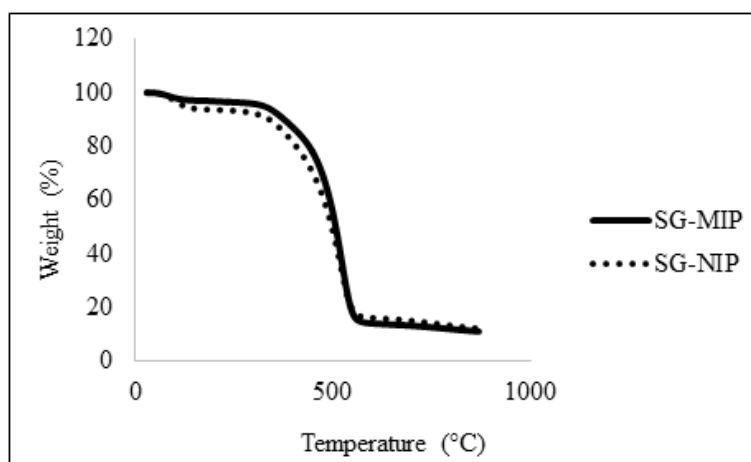
FIGURE 3. Morphological images of SG-MIP and SG-NIP

SURFACE AND POROSITY ANALYSIS

Table 1 tabulates the surface and porosity values of SG-MIP and SG-NIP. The resulting values for SG-MIP are greater than those of SG-NIP. This determined that the presence of a template on the SG-MIP designed a cavity and confined a shrinkage of pores effectively in the polymerization process. This finding could allow that the SG-MIP has higher adsorption capacity and better pores formation than those of the SG-NIP.

TABLE 1. Surface and porosity result of SG-MIP and SG-NIP

Polymers	Surface area (m^2g^{-1})	Pore diameter (nm)	Pore volume (μm)
SG-MIP	10.65	6.03	160.63
SG-NIP	3.92	3.30	2.94

SELECTIVITY ANALYSIS

The selective binding experiment was carried out towards SG-MIP by comparing it with SG-NIP. Figure 4 performs that the selectivity and affinity performance of SG-MIPis better than SG-NIP. However, SG-MIP has a better selectively adsorbent for CV than methylene blue (MB). MB was chosen as competitor due to this similar structure with CV which both of them are cationic dye (El-Sayed 2011). MB and CV both are cationic dye. This result proves the selectivity and affinity performance of SG-MIP are better than SG-NIP due to specific recognition sites of CV molecule left on the SG-MIP matrix network but non-specific recognition on the SG-NIP matrix. The formation of complementary spatial structure for the selective recognition of the CV template on SG-MIP was also identified. The adsorption of MB (which is one of the similar structurally with CV) on SG-MIP suggested the existence of cross-binding reactivity. This cross-binding reactivity has an advantage in sample treatment due to template analogues class could be also removed or enriched efficiently (Asman et al. 2015a; Fang et al. 2011; Vasapollo et al. 2011; Zakaria et al. 2009).
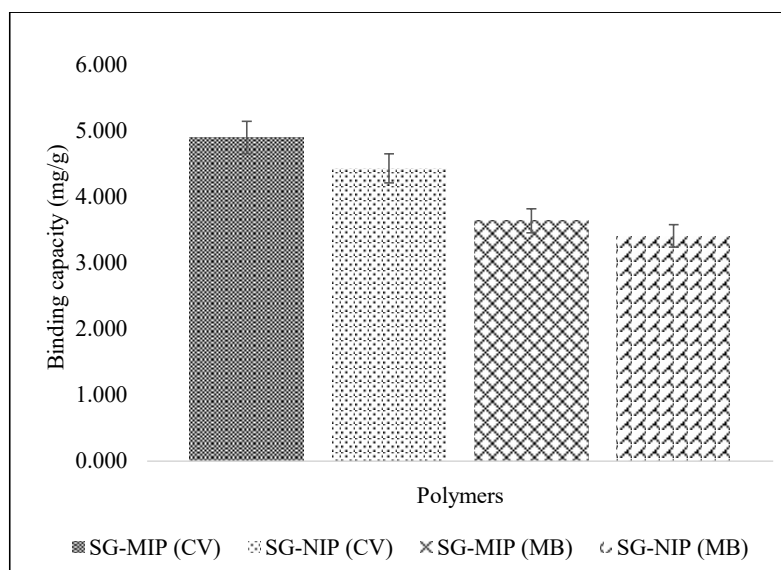
FIGURE 4. Binding specificity study

KINETIC STUDY

Figure 5 illustrates the similar curves of adsorption kinetic towards CV for SG-MIP and SG-NIP. The sorption process is rapid at 5 min and gradually increased at 15 min, and remained stable after 15 min. The rapid sorption of CV at an early stage was credited to the express binding of CV molecules on the surface of SG-MIP and SG-NIP. It is caused by the large numbers of a vacant surface site on polymers with a high concentration of CV analyte. After a certain time at 15 min and after, the remaining vacant surface site was difficult to occupy because of the repulsive forces between CV solute molecules on the polymers surface phase. Hence, the uptake of CV reaches equilibrium (Asman et al. 2016).

Figure 6 shows the pseudo first order model and Figure 7 presents the pseudo second order model. The resulting graphs are summarized in Table 2. It showed the pseudo-second order model well fits the kinetic adsorption over pseudo-first order model based on R_2 values nearly 1, for SG-MIP and SG-NIP. Moreover, the

calculated $q_{e,\,cal}$ value of SG-MIP, and SG-NIP are found closer to the experimental uptake values of $q_{e,exp}$ SG-MIP, and SG-NIP, respectively. The adsorption system did not agree with the pseudo-first order model, because the calculated $q_{e,\,cal}$ value of SG-MIP and SG-NIP did not give practical values and too low with regards to the experimental values, $q_{e,exp}$ (mgg^{-1}). Further, the R_2 value is below 0.9 far from 1 (Abbas et al. 2020; Miyah et al. 2017). Meanwhile, the high initial sorption rate, h (mgg^{-1} min), and low values of time necessary for the adsorption at t$_{1/2}$ proved that the MIP-SG is good polymer adsorbent than NIP-SG (Asman et al. 2015b). This occurs owing to the occurrence of imprinting effect in the interior surface of MIP-SG, which results in broader pore diameter and lower pore volume for the MIP-SG matrix, verifying the super pore enhancement of mass transport for CV analyte. The adsorption kinetic was primarily well-ordered by the pore structure of adsorbents. Additionally, the faster mass transfer performance was occurred due to small diffusion distance transport which was affected by the board pore structures.
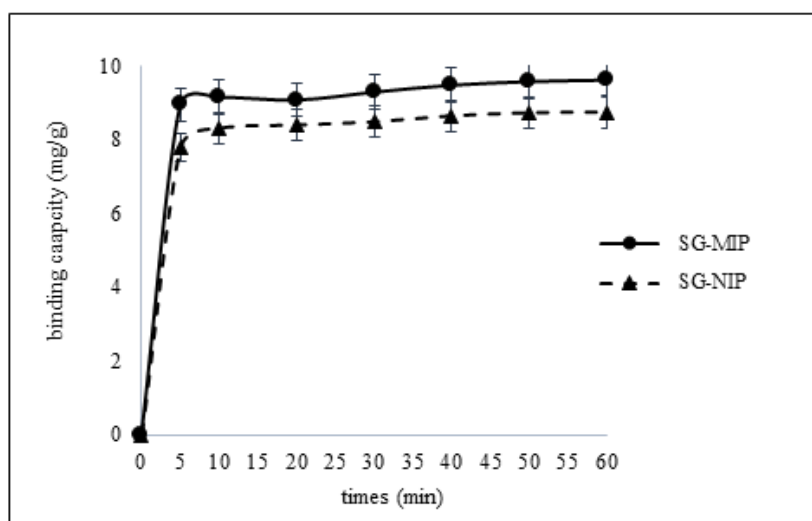
FIGURE 5. Kinetic study
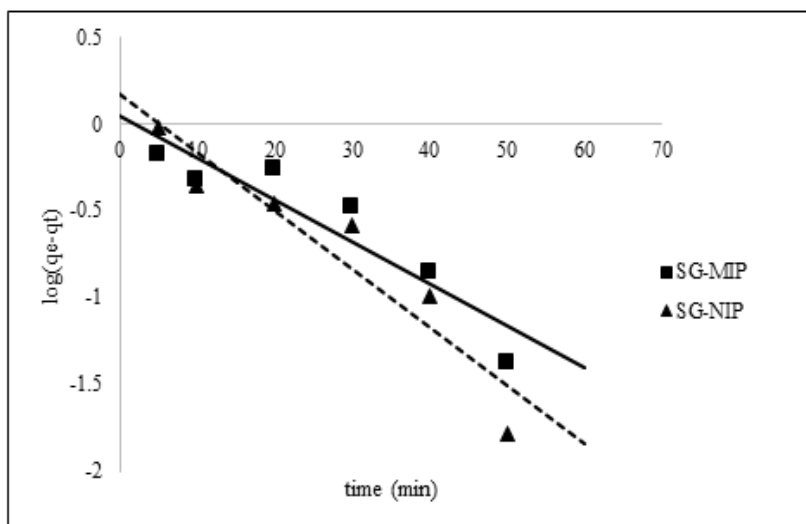
FIGURE 6. Pseudo first order model
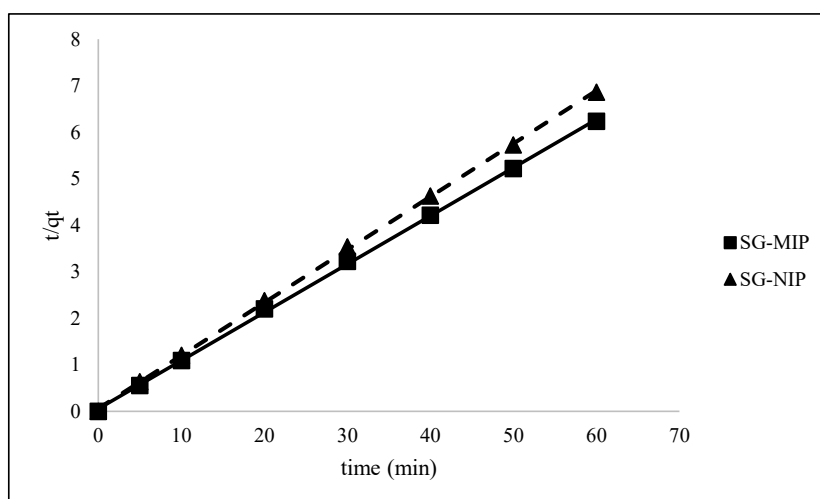
FIGURE 7. Pseudo second order model

TABLE 2. Kinetic parameters for the adsorption of CV on SG-MIP and SG-NIP

Kinetic model	Parameter	SG-MIP	SG-NIP
	$q_{e,exp}$ (mgg^{-1})	9.0853	8.3964
Pseudo-first order	$q_{e,\,cal}$ (mgg^{-1})	1.1092	1.4791
	k_1 (min^{-1})	0.0557	0.0829
	R^2	0.8600	0.8894
Pseudo-second order	$q_{e,\,cal}$ (mgg^{-1})	9.6525	8.7951
	h	17.0648	15.3139
	k_2 (gmg^{-1} min^{-1})	0.1832	0.1980
	R^2	0.9996	0.9997
	$t_{1/2}$	0.0586	0.0653

ISOTHERM STUDY

The sorption isotherm study of MIP-SG and NIP-SG were studied through several concentrations. The binding isotherm of crystal violet shows that the amount of crystal violet bound to MIP-SG and NIP-SG is increased with increasing concentration until it achieved a saturation level at 10 mgL^{-1} and later decreased afterward (Figure 8). However, the concentration adsorption of NIP-SG is lower than MIP-SG. This indicate that the SG-MIP has specific cavity towards CV. Similar trend was found by Kudupoje et al. (2018).

Langmuir and Freundlich isotherm models graphs for MIP-SG and NIP-SG are exhibited in Figures 9 and 10. Table 3 summarizes the findings result for isotherm adsorption studies. Table 2 shows that $q_{m, cal}$ and the Langmuir constant values (b) values of MIP-SG are higher than the NIP-SG indicated that SG-MIP has a better affinity and strongly improved the binding sites better than NIP-SG. Furthermore, the R^2 value exposed that the Langmuir isotherm model seems to deliver better fitting (R^2 value is above 0.9 and nearly 1), confirming the adsorption system of MIP-SG and NIP-SG is homogeneous. Besides, R$_L$ values are in the range 0 to 1, demonstrating that the adsorption mechanism is encouraging over the range of initial CV concentrations (Narwade et al. 2017). Then, the degree of favorability for MIP-SG is superior to NIP-SG.

Meanwhile, by Freundlich isotherm data, the K$_f$ value of SG-MIP is higher than SG-NIP indicated a greater adsorption capacity of SG-MIP. Furthermore, the Freundlich isotherm model of R^2 value shows better fitting (R^2 value is above 0.9 and nearly 1), thus confirming the heterogeneous binding sites. Besides, the sorption process is more favorable due to the n and 1n^{-1} values are above and less than 1, respectively. It also inferred that adsorption CV on SG-MIP is more favorable than SG-NIP with better adsorption towards CV because the higher n values of SG-MIP indicate the strong bonds formed between the adsorbate and adsorbent. When compared to the R^2 value, it can be seen that the Freundlich model is best fitted over the Langmuir model.

Figure 11 shows the Scatchard plot for the rebinding study of SG-MIP and SG-NIP. The Scatchard plot was studied to approximate the binding properties of the polymers. The Scatchard plot is a simple guideline to identify multiple classes of binding sites. As seen in Figure 11, Scatchard plots of SG-MIP and SG-NIP are not a single linear curve but comprises of two linear parts with dissimilar slopes. It could be summarized that the binding site configuration of the SG-MIP and SG-NIP is heterogeneous. It also shows that the binding sites could be categorized into two distinct groups with dissimilar specific binding properties. The origin of molecular recognition in polymers is normally credited to the shape selectivity and the pre-organization of functional groups. Nevertheless, the shape selectivity was also affected by functional group pre-organization in MIPs (Okutucu et al. 2010). The Scatchard plots support the Freundlich model study.
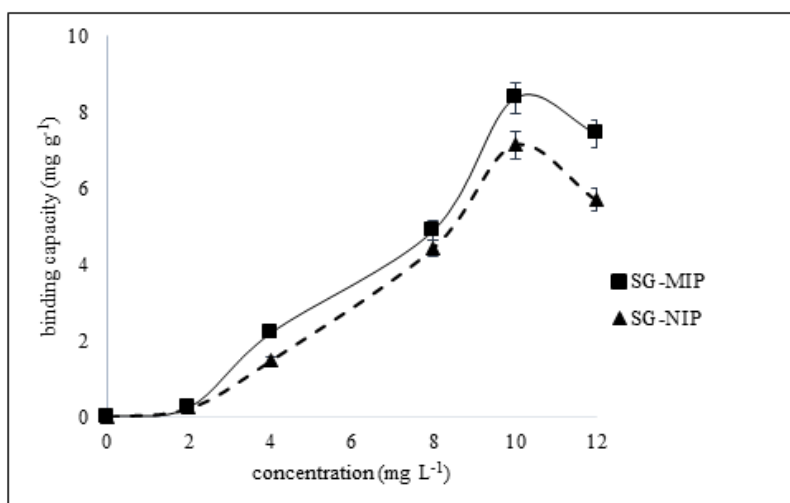
FIGURE 8. Isotherm study
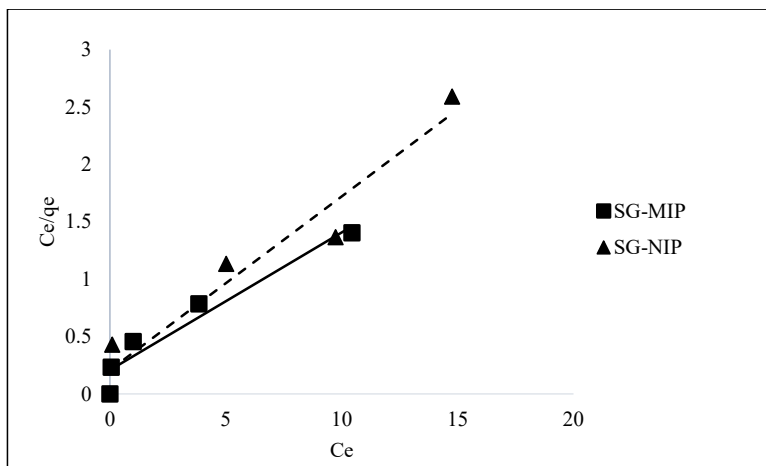
FIGURE 9. Langmuir model

$$y = 0.6756x + 0.2096$$
$$R^2 = 0.95$$
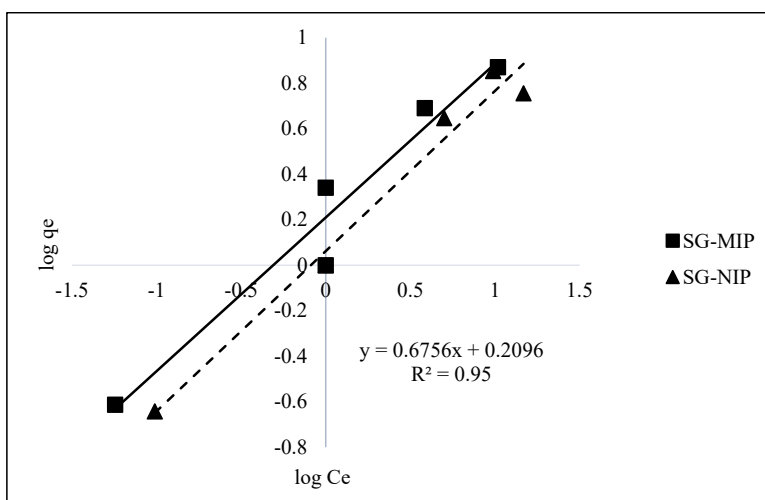
FIGURE 10. Freundlich model

(a)

(b)
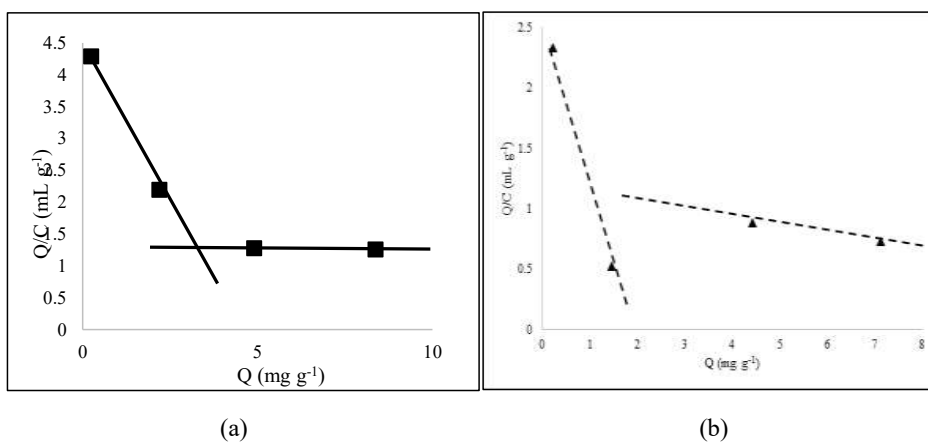
FIGURE 11. Scatchard plot (a) SG-MIP and (b) SG-NIP

TABLE 3. Isotherm parameters for the adsorption of CV on SG-MIP and SG-NIP

Adsorption model	Parameter	SG-MIP	SG-NIP
Langmuir	$q_{m,exp}$ (mgg^{-1})	8.3704	7.1357
	$q_{m,cal}$ (mgg^{-1})	8.3403	6.6138
	b (Lmg^{-1})	0.5776	0.7294
	R_L	0.1479	0.1206
	R^2	0.9362	0.9405
Freundlich	$q_{e,cal}$ (mgg^{-1})	12.6432	8.7770
	K_f (mg^{1-m} L^m g^{-1})	1.6203	1.1548
	n	1.4802	1.4207
	$1/n$	0.6756	0.7039
	R^2	0.9500	0.9764

CONCLUSION

The sol-gel molecularly imprinted polymer (SG-MIP) for the selective recognition of crystal violet was well studied. The FTIR result presented that the SG-MIP and SG-NIP were successfully prepared. The morphological observation exhibited rough, densely packed, loose, and porous surfaces for SG-MIP. Differ with SG-NIP which presence rougher, pores, and less dense. The surface and porosity values of SG-MIP are greater compared to SG-NIP, thus indicating the influence of the adsorption capacity of SG-MIP is more favourable than SG-NIP. The result also indicates that the SG-MIP has considerable potential for better selectivity and affinity towards CV compared to SG-NIP, which was supported by the characterization study. The adsorption capacity of CV was greater on the SG-MIP over SG-NIP. The kinetic study presented that the pseudo second order model was well close-fitting with a higher correlation for the adsorption of CV. The isotherm study was showed that the Freundlich model was selected as best fitted compared to Langmuir which was supported by the Scatchard plot. Conclude that, the sol-gel method gives a promising alternative to molecular imprinting technology, not only proposes ease method but also enhances the physical and chemical properties of MIP.

ACKNOWLEDGEMENTS

REFERENCES

Abbas, M., Harrache, Z. & Trari, M. 2020. Mass-transfer processes in the adsorption of crystal violet by activated carbon derived from pomegranate peels: Kinetics and thermodynamic studies. *Journal of Engineered Fibers and Fabrics* https://doi.org/10.1177%2F1558925020919847.

Asman, S., Mohamad, S. & Sarih, N.M. 2016. Study of the morphology and the adsorption behavior of molecularly imprinted polymers prepared by reversible addition-fragmentation chain transfer (RAFT) polymerization process based on two functionalized β-cyclodextrin as monomers. *Journal of Molecular Liquids* 214: 59-69.

Asman, S., Mohamad, S. & Sarih, N.M. 2015a. Exploiting β-cyclodextrin in molecular imprinting for achieving recognition of benzylparaben in aqueous media. *International Journal of Molecular Sciences* 16(2): 3656-3676.

Asman, S., Mohamad, S. & Sarih, N.M. 2015b. Influence of polymer morphology on the adsorption behaviors of molecularly imprinted polymer-methacrylic acid functionalized β-cyclodextrin. *Journal of Applied Polymer Science* 132(43): 42720.

Binupriya, A.R., Sathishkumar, M., Ku, C.S. & Yun, S.I. 2010. Biosorption of procion red mx 5b by *Bacillus subtilis* and its extracellular polysaccharide: Effect of immobilization. *CLEAN - Soil, Air, Water* 38(8): 775-780.

El-Sayed, G.O. 2011. Removal of methylene blue and crystal violet from aqueous solutions by palm kernel fiber. *Desalination* 272(1): 225-232.

Ertürk, G. & Mattiasson, B. 2017. Molecular imprinting techniques used for the preparation of biosensors. *Sensors* 17(2): 288.

Esfandian, H., Jafari, M., Alizadeh, M., Rahmati, H.T. & Katal, R. 2012. Synthesis of polyaniline nanocomposite and its application for chromium removal from aqueous solution. *Journal of Vinyl and Additive Technology* 18(4): 250-260.

Fang, L., Chen, S., Zhang, Y. & Zhang, H. 2011. Azobenzene-containing molecularly imprinted polymer microspheres with photoresponsive template binding properties. *Journal of Materials Chemistry* 21(7): 2320-2329.

Kessler, V.G. 2018. The synthesis and solution stability of alkoxide precursors. In *Handbook of Sol-Gel Science and Technology: Processing, Characterization and Applications*, edited by Klein, L., Aparicio, M. & Jitianu, A., Cham: Springer International Publishing. pp. 31-80.

Kia, S., Fazilati, M., Salavati, H. & Bohlooli, S. 2016. Preparation of a novel molecularly imprinted polymer by the sol-gel process for solid phase extraction of vitamin D3. *RSC Advances* 6(38): 31906-31914.

Kudupoje, M.B., Klotz, J.L., Yiannikouris, A., Dawson, K.A., McLeod, K.R. & Vanzant, E.S. 2018. Contractile response of bovine lateral saphenous vein to ergotamine tartrate exposed to different concentrations of molecularly imprinted polymer. *Toxins* 10(2): 58.

Kulkarni, M.R., Revanth, T., Acharya, A. & Bhat, P. 2017. Removal of crystal violet dye from aqueous solution using water hyacinth: Equilibrium, kinetics and thermodynamics study. *Resource-Efficient Technologies* 3(1): 71-77.

Kumar, R. & Ahmad, R. 2011. Biosorption of hazardous crystal violet dye from aqueous solution onto treated ginger waste (TGW). *Desalination* 265(1-3): 112-118.

Lellis, B., Fávaro-Polonio, C.Z., Pamphile, J.A. & Polonio, J.C. 2019. Effects of textile dyes on health and the environment and bioremediation potential of living organisms. *Biotechnology Research and Innovation* 3(2): 275-290.

Miyah, Y., Lahrichi, A., Idrissi, M., Boujraf, S., Taouda, H. & Zerrouq, F. 2017. Assessment of adsorption kinetics for removal potential of crystal violet dye from aqueous solutions using Moroccan pyrophyllite. *Journal of the Association of Arab Universities for Basic and Applied Sciences* 23: 20-28.

Narwade, V., Kokol, V. & Khairnar, R. 2017. Phenol adsorption on graphite-hydroxyapatite nanocomposites: Kinetic and isotherm study. *Journal of Materials Science and Surface Engineering* 5(2): 544-548.

Okutucu, B., Akkaya, A. & Pazarlioglu, N.K. 2010. Molecularly imprinted polymers for some reactive dyes. *Preparative Biochemistry & Biotechnology* 40(4): 366-376.

Torres-Caban, R., Vega-Olivencia, C.A. & Mina-Camilde, N. 2019. Adsorption of Ni2+ and Cd2+ from water by calcium alginate/spent coffee grounds composite beads. *Applied Sciences* 9(21): 4531. https://www.mdpi.com/2076-3417/9/21/4531

Vasapollo, G., Sole, R.D., Mergola, L., Lazzoi, M.R., Scardino, A., Scorrano, S. & Mele, G. 2011. Molecularly imprinted polymers: Present and future prospective. *International Journal of Molecular Sciences* 12(9): 5908-5945.

Wang, L., Zhi, K., Zhang, Y., Liu, Y., Zhang, L., Yasin, A. & Lin, Q. 2019. Molecularly imprinted polymers for gossypol via sol-gel, bulk, and surface layer imprinting - A comparative study. *Polymers* 11(4): 602.

Zakaria, N.D., Yusof, N.A., Haron, J. & Abdullah, A.H. 2009. Synthesis and evaluation of a molecularly imprinted polymer for 2,4-dinitrophenol. *International Journal of Molecular Sciences* 10(1): 354-365.

Saliza Asman* & Mohd Kamarulzaki Mustafa
Department of Physics and Chemistry
Faculty of Applied Sciences and Technology
Universiti Tun Hussein Onn Malaysia
Education Hub Pagoh
84600 Pagoh, Johor Darul Takzim
Malaysia

Sharifah Mohamad
Department of Chemistry
Faculty of Science
University of Malaya
Lembah Pantai, 50603 Kuala Lumpur, Federal Territory
Malaysia

*Corresponding author; email: salizaa@uthm.edu.my